iScience

CellPress
OPEN ACCESS

Article

H_2SO_4 assisted hydrothermal conversion of biomass with solid acid catalysis to produce aviation fuel precursors

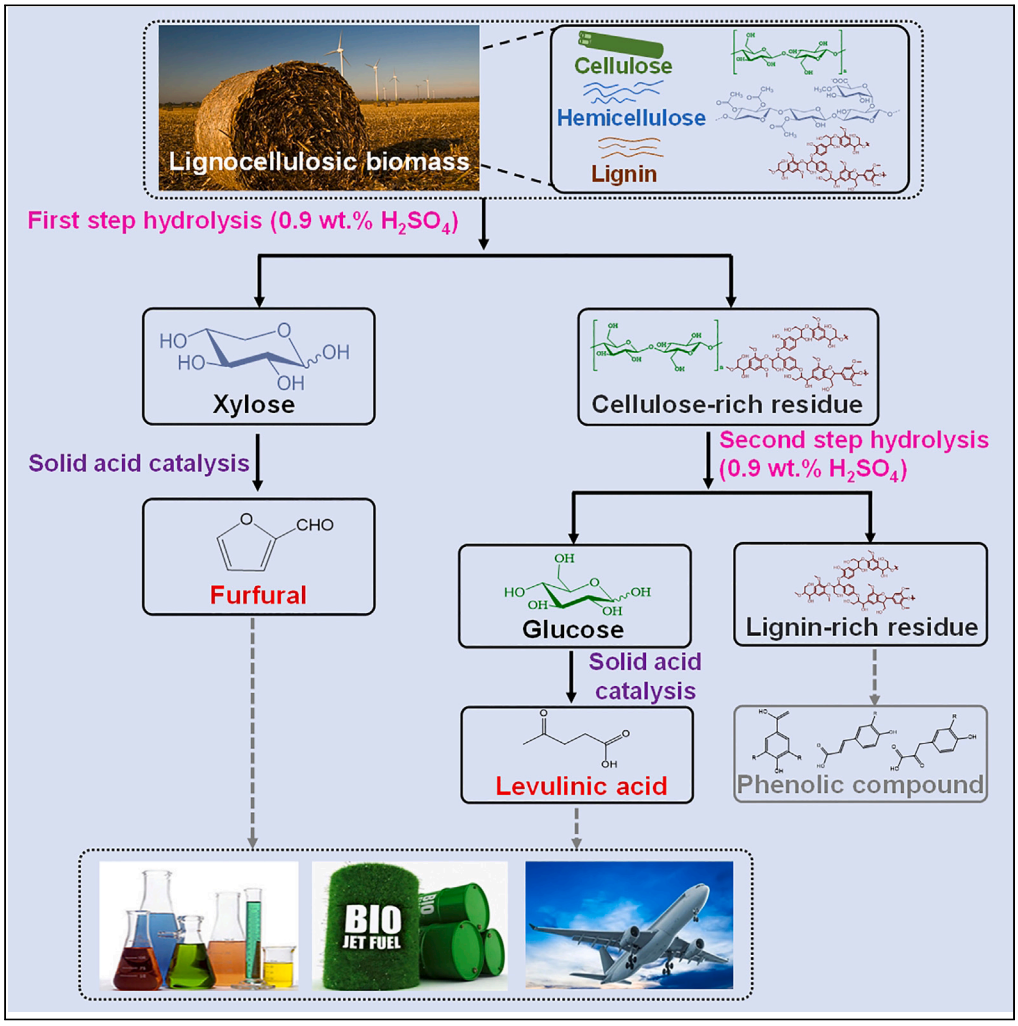

Lingjun Zhu, Hao Xu, Xiaoyan Yin, Shurong Wang

srwang@zju.edu.cn

Highlights

A Novel method of biomass conversion was proposed for production of FF and LA

A very low concentration of H_2SO_4 was used in the hydrolysis of biomass

Solid acid catalyst with skeleton itself containing sulfonic acid group was prepared

The solid acid catalyst exhibited high catalytic performance in 28 catalytic runs

Zhu et al., iScience 26, 108249
November 17, 2023
https://doi.org/10.1016/j.isci.2023.108249

iScience

CellPress
OPEN ACCESS

Article

H_2SO_4 assisted hydrothermal conversion of biomass with solid acid catalysis to produce aviation fuel precursors

Lingjun Zhu,[1] Hao Xu,[1] Xiaoyan Yin,[1] and Shurong Wang[1,2,*]

SUMMARY

With hydrothermal reaction, lignocellulosic biomass can be efficiently converted into furfural (FF) and levulinic acid (LA), both of which are key platform compounds that can be used for the subsequent preparation of aviation fuels. In order to reduce the acid concentration in traditional hydrolysis and provide a reaction system with good catalytic activity, we propose a biomass conversion route as dilute acid hydrolysis coupled with solid acid catalysis. Firstly, at different temperatures, the hemicellulose and cellulose in corn stover were step-hydrolyzed by sulfuric acid solution with a concentration of 0.9 wt. % to produce xylose and glucose, with conversion reaching 100% and 97.3%, respectively. Subsequently, a new resin-derived carbon-based solid acid catalyst was used to catalyze the aforementioned saccharide solutions to obtain FF with yield of 68.7 mol % and LA of 70.3 mol %, respectively. This work provides a promising approach for the efficient production of bio-aviation fuel precursors.

INTRODUCTION

With the sharp increase in global consumption of fossil fuels, the price of traditional energy continues to rise, and the pressure of carbon emission reduction is gradually increasing. The use of renewable resources such as biomass to produce carbon-neutral or low-carbon-emission fuels is becoming increasingly crucial in replacing traditional fossil fuels. Meanwhile, new directions and novel proposals for cost-effective and green-like biomass conversion have received extensive attention from researchers.[1,2] Corn stover has a large yield and contains more than 30% carbohydrates, how to use it with high efficiency and low cost has become a research hotspot in the field of biomass utilization. The general way to use this biomass is to convert cellulose into ethanol. Wu et al.[3] performed two green-like pretreatments (20 min liquid hot water, 15% CaO at 50°C) on corn brittle stalk, and the results showed that the accessibility of cellulose was significantly improved, the biomass enzymatic saccharification was almost completely realized, and the bioethanol yield reached 19.3%. Recently, it was found that hydrothermal conversion can convert biomass into high-purity platform chemicals such as furfural (FF), 5-hydroxymethylfurfural (HMF), and levulinic acid (LA).[4,5] It is an efficient catalytic conversion pathway to achieve target products with high selectivity.

Inorganic acid catalysts are extensively applied in the hydrothermal conversion of biomass. The majority of plants use high-concentration H_2SO_4 (10–25 wt. %) as a catalyst to produce FF at a large scale, for instance, in the BIOFINE process.[6] However, the use of high-concentration homogeneous inorganic acids as catalysts may result in the final reaction mixtures containing high concentrations of inorganic acids. This can cause severe environmental pollution, making it essential to separate the product from these mixtures. Recent studies have shown that ionic liquid catalysts have garnered increasing attention due to their excellent catalytic performance. Ramli et al.[7] utilized an acidic ionic liquid, [SMIM][$FeCl_4$] to convert oil palm leaves, resulting in a 59 mol % LA yield. Zhou et al.[8] utilized [C_4MIM][HSO_4] ionic liquid as a catalyst to convert bamboo shoot shell at 145°C and obtained 71 mol % LA yield. Novodárszki et al.[9] studied the conversion of sweet sorghum straw to LA in an ionic liquid catalytic system, where the raw material was first pretreated in 2 mol/L H_2SO_4 for 20 min. The highest LA yield of 67 mol % was obtained after the reaction with microwave heating at 160°C for 30 min, and this method can also be used to produce 5-HMF. Zhao et al.[10–13] systematically investigated various Brønsted/Lewis acidic ionic liquid catalysts for catalyzing the hydrothermal conversion of xylose, xylan, and straw to FF in a water-butanone-mixed solvent system. Their results showed that $FeCl_3$ contributed to the isomerization process of xylose to xylulose and that an appropriate amount of butanone could increase FF yield. When the volume ratio of butanone to water was 4:1, the FF yield reached 51 mol %. However, despite the high target product yield obtained with ionic liquid catalysis, its practical use is greatly limited by the high preparation cost and the low recycling performance.

Compared to homogeneous inorganic acid or ionic liquid catalysts, heterogeneous catalysts have better resistance to impurities and a longer recycling life.[14] However, in direct hydrothermal conversion of biomass, separating the heterogeneous catalyst from the depolymerization residue is often difficult. As a result, these catalysts are mainly used to convert the soluble monosaccharides or oligosaccharides

[1]State Key Laboratory of Clean Energy Utilization, Zhejiang University, Hangzhou 310027, China
[2]Lead contact
*Correspondence: srwang@zju.edu.cn
https://doi.org/10.1016/j.isci.2023.108249

produced from the primary degradation of biomass. Li et al.[15] synthesized a tin-loaded montmorillonite (Sn-MMT) solid acid catalyst for xylose and xylan conversion experiments. The conversion of xylose was 76.8 mol %, and the FF yield was 52.5 mol % after 30 min reaction at 180°C in an H_2O/NaCl-dimethyl sulfoxide biphasic system. Gupta et al.[16] investigated the preparation of FF from xylose catalyzed by Nb_2O_5 with Brønsted/Lewis acid sites. They discovered that using toluene as an extractant can increase FF selectivity from 48 mol % to 72 mol % and that the Lewis acid activity was reduced by loading humins.

Carbon-based solid acid catalysts are widely used in the hydrothermal conversion of biomass due to their excellent hydrothermal stability and catalytic activity.[17] The preparation of carbon-based catalysts from biomass and its derived materials has become a research hotspot due to its comprehensive source and environmental friendliness. Wang et al.[18] prepared a solid acid catalyst by sulfonating the carbon support obtained from the pyrolysis of Chinese silvergrass. Using this catalyst, the FF yields in the process of xylose and xylan conversion were 60 mol % and 42 mol %, respectively, after 60 min of reaction at 190°C. Shen et al.[19] developed a novel sulfonated commercial charcoal solid acid catalyst using a one-pot method with *p*-toluenesulfonic acid sulfonation. The catalyst, rich in acid sites contributed by sulfonic acid, carboxylic acid, and phenolic hydroxyl acid, exhibited high catalytic activity in the dehydration of xylose to FF, yielding 72.1 mol % FF after 60 min of reaction at 140°C in tetrahydrofuran/dimethyl sulfoxide solvent. No significant reduction in catalyst activity was observed after five catalytic runs. Gan et al.[20] prepared hydrothermal carbon using an alkali lignin pretreated with acrylic acid and then synthesized a catalyst through sulfuric acid sulfonation. They discovered that more −COOH groups (2.85 mmol/g) contributed to the activity of the $-SO_3H$ groups (1.58 mmol/g) as the primary catalytic active sites.

To enhance the homogeneity and structural stability of carbon-based solid acid catalysts, Zhu et al.[21] prepared a resorcinol-formaldehyde resin carbon catalyst (RFC) with an ordered mesoporous skeleton through a soft template method. They synthesized a sulfonated carbon-based solid acid catalyst (S-RFC) using *p*-aminobenzenesulfonic acid as the sulfonating agent at ambient temperature. The catalyst had a uniform structure, high surface acid concentration, and excellent hydrothermal stability. The concentration of $-SO_3H$ in the catalyst was 0.86 mmol/g, and the specific surface area was 530 m^2/g. At 170°C after 15 min of xylose dehydration, the FF yield was 80 mol %. Although resin-based carbon solid acids have higher hydrothermal stability and a more uniform structure than conventional amorphous carbon-based solid acids, they are sulfonated in the same manner. After synthesizing the skeleton structure, a separate sulfonation step is still required to obtain acid sites for the solid acid. The strongly acid sites obtained by sulfonation are susceptible to shedding during the hydrothermal conversion process, leading to decreased catalyst activity.

To achieve good performance in the hydrothermal conversion of lignocellulosic biomass to obtain FF and LA, the research focused not only on the development of novel catalyst but also on studying the reaction pathway. On one hand, FF and *p*-hydroxybenzenesulfonic acid (PHSA) were utilized as substrates for the synthesis of a resin-derived solid acid catalyst, wherein the skeleton itself containing sulfonic acid groups. On the other hand, to address the issues of high acid concentration in traditional acid hydrolysis processes and difficulties in separating the catalyst in hydrothermal conversion of biomass catalyzed by solid acid, a new reaction system combining dilute acid hydrolysis with solid acid catalytic conversion was proposed. In this reaction system, the concentration of sulfuric acid used for biomass hydrolysis was reduced to less than 1 wt. %, making it less corrosive to equipment.

RESULTS AND DISCUSSION

TG/DTG

Thermal stability of both fresh and used catalysts was assessed using TG analysis, and the results are shown in Figure 1. The thermal weight-loss range of the fresh catalyst remains continuous after 447°C, and the corresponding DTG curve represents a narrow weight-loss peak. This

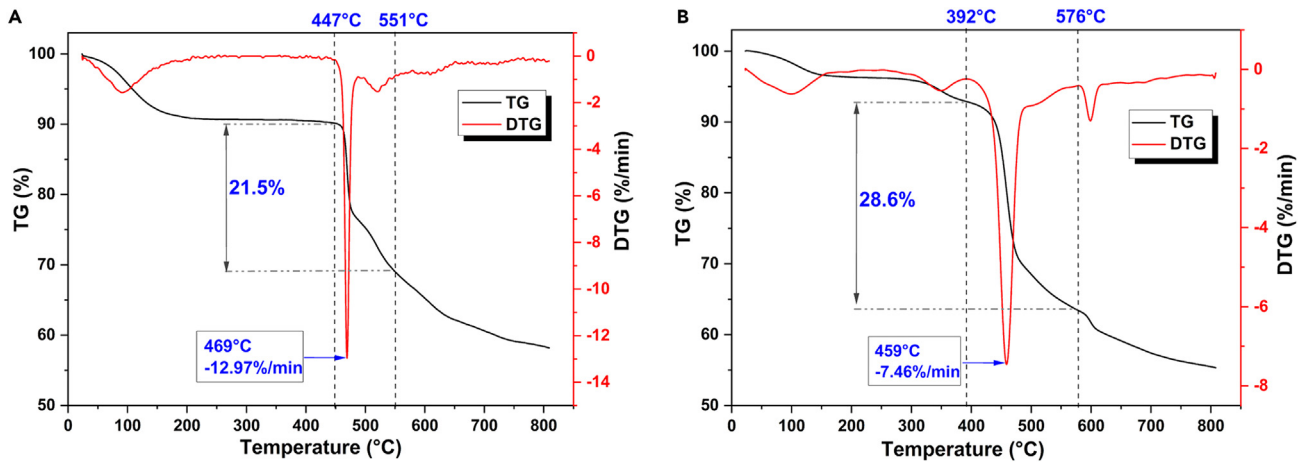

Figure 1. TG/DTG of fresh and used catalysts

(A) Fresh catalyst.

(B) Used catalyst after 28 catalytic runs.

suggests that the catalyst exhibits high thermal stability under hydrothermal temperatures (150°C–250°C). The superior thermal stability can be attributed to the catalyst's main structure, which comprises furan and benzene rings linked by C-C bonds. Both ring structures demonstrate excellent thermal stability and are hardly decomposed under temperatures below 300°C. With increasing temperature, the sulfonic acid functional group gradually dissociates, and this process is accompanied by ring opening and dehydration carbonization of the furan ring, leading to a continuous weight loss of the catalyst.[22]

As shown in Figure 1, the maximum weight-loss rate of the fresh catalyst occurs at 469°C, which is higher than that of the carbon-based solid acids prepared by sulfonation using biomass as the carbon source.[23] The thermal weight-loss range of the used catalyst is observed after 390°C, indicating that the used catalyst still possesses good thermal stability. Compared with catalyst-01, the initial temperature of thermal weight-loss of catalyst-28 decreases slightly from the original 447°C to 392°C, and its corresponding DTG curve shows a broader weight-loss peak caused by the decomposition of the humins that are enriched on the catalyst surface. Wang et al.[24] found that this class of humins has an unstable branched structure by analyzing the thermodynamic behavior of sugar-derived humins, resulting in its decomposition at lower temperatures. This corroborates the slight reduction in the temperature corresponding to the maximum thermal weight-loss rate of the used catalyst (459°C) compared to that for the fresh catalyst (469°C).

FTIR

Figure 2 shows the FTIR results of both the fresh and used catalysts. Similar characteristics can be observed in the distribution of functional groups for both the fresh catalyst and the used catalyst after 28 catalytic runs. The solid acid catalyst is composed of FF and PHSA units through aldol condensation, resulting in distinctive O-H stretching vibration peaks of phenolic and aliphatic hydroxyl groups (centered at 3,650 cm^{-1}), as well as aromatic/aliphatic C-H peaks contributed by methyl, methylene, and methylate structures (centered at 2,945 cm^{-1}). The FTIR results also revealed sulfonic acid groups on solid acid catalysts, indicated by the vibrational peaks at 1225, 1170, and 1,035 cm^{-1}, which correspond to the characteristic peaks of sulfonic acid groups ($-SO_3H$).[25–27] Although the intensity of the corresponding peaks for the used catalyst was slightly weakened compared to the fresh catalyst, the overall distribution of both characteristic peaks remained the same, indicating that the recycling process did not significantly affect the main structure of the catalyst. This, in combination with the TG/DTG analysis, suggests that the catalyst is highly stable under hydrothermal conversion conditions.

Elemental composition and surface acid concentration

Table 1 shows the element and surface acid concentrations (SACs) of fresh, used, and regenerated catalysts at different stages of the cycling process. The initial S content for catalyst-01 is 13.10 wt. %, which correlates to a SAC of 2.63 mmol/g, suggesting that the sulfonic acid functional groups are accessible on the catalyst surface during the synthesis—a desirable characteristic for subsequent catalytic reactions. During the first reaction period, the S content reduces from 13.10 wt. % to 9.73 wt. %, decreasing the corresponding SAC from 2.63 mmol/g to 0.85 mmol/g. This trend remains consistent throughout the three reaction periods that follow. Therefore, it can be deduced that after every reaction period, there is gradual accumulation of depolymerization residue on the catalyst surface and in the channels and minor loss of sulfonic acid functional groups. These factors lead to a gradual increase in carbon content of the catalyst, which coincides with the gradual decrease in S content, as observed in the change of SACs for the catalysts. Regeneration of the catalysts after a reaction period can restore the S content and SACs to their initial values.

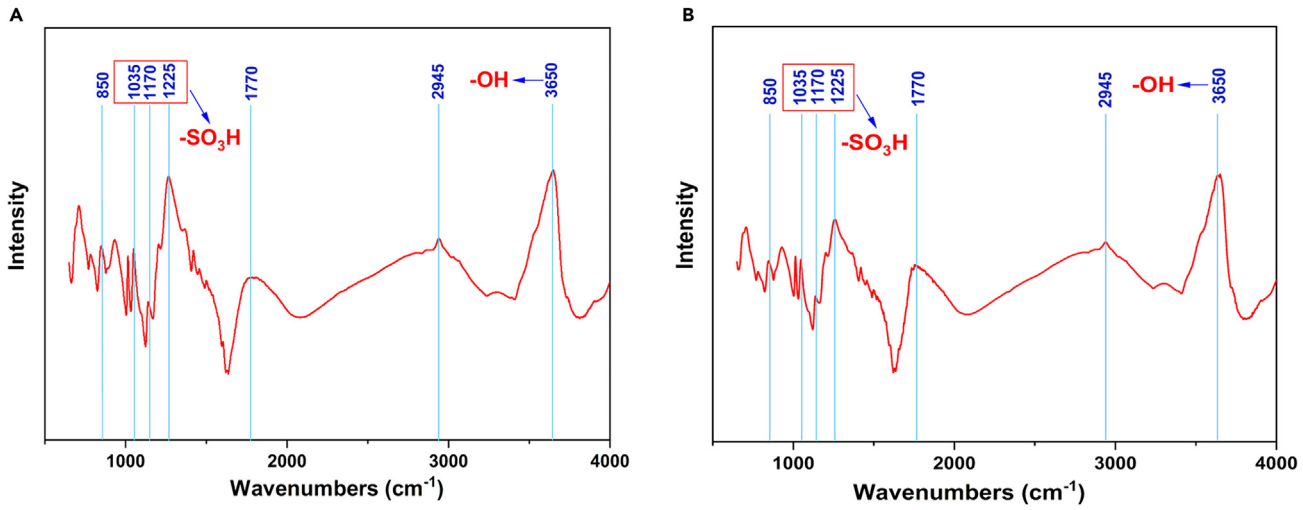

Figure 2. FTIR of fresh and used catalysts

(A) Fresh catalyst.

(B) Used catalyst after 28 catalytic runs.

Table 1. Element and SACs of the fresh, used and regenerated catalysts

Catalysts	C (wt. %)	H (wt. %)	O (wt. %)	S (wt. %)	SAC (mmol/g)
01	59.49	4.66	21.74	13.10	2.63
07	60.57	4.61	25.09	9.73	0.85
08	52.46	4.69	31.44	11.41	2.17
14	61.66	4.85	23.81	9.67	0.29
15	58.26	4.72	25.54	11.46	1.97
21	61.03	4.59	24.37	10.01	0.38
22	55.39	4.68	27.57	12.36	2.87
28	62.37	5.42	21.82	10.38	0.56

Table 2 listed the pore structure of the fresh, used, and regenerated catalysts. Compared to catalysts with a small-pore structure, this large-pore structure was more favorable for the contact between substances and the acid sites within the catalyst. The larger pore size can facilitate the separation of solid by-product humins produced during the hydrothermal conversion process, resulting in high catalytic activity and recycling performance for catalyst.[28] During the sulfonation process, the humins were adequately decomposed and separated from the catalyst during the subsequent washing process. The sulfonation process also compensated for the loss of some sulfonic acid functional groups from the catalyst during recycling, thus restoring the catalytic activity to its initial state. Although the surface area, average pore size, and most probable pore size of the catalyst decreased to varying degrees during the recycling process, simple regeneration significantly improved these parameters and brought them close to their initial levels. Therefore, regeneration of the used catalysts was a necessary and reliable step.

Surface morphology

As shown in Figure 3, the surface of the used catalysts before regeneration was covered predominantly with insoluble residues, which resulted in pore blockage, deactivation of surface acidic sites, and decreased catalytic activity. This was further supported by the results of SACs and BET surface areas. In contrast, regeneration of the catalysts removed most of the depolymerization residues present on the surface, leading to an increase in its specific surface areas and SACs.

Figure 4 shows the EDS mapping of C, S, and O in the catalysts before and after recycling. The dispersion of these elements appears relatively homogeneous, with uniform distribution observed in both catalysts. Combined with the results of elemental analysis, it can be inferred that the main reason for the decrease in S element content is due to the aggregation of humins produced from the catalytic reaction process. The basic structure of humins produced from hydrothermal conversion of biomass is an insoluble polymer composed of furan and aromatic rings connected by aliphatic carbon chains, which contain C, H, and O. Therefore, the aggregation of humins results in an increase in the relative content of C, H, and O in the catalyst and a decrease in S.

First step hydrolysis for the conversion of hemicellulose to xylose

The hemicellulose fraction of lignocellulosic biomass is a heterogeneous polymer composed of xylose and several other monosaccharides (e.g., arabinose, galactose, etc.). As xylose is the predominant product in hydrolysis, the impact of reaction conditions on xylose yield was investigated. The xylose yields and hemicellulose conversions in the hydrolysis of corn stover to xylose-rich hydrolysate at varying temperatures are shown in Figure 5. At the same reaction temperature, the yield of xylose initially increased and subsequently decreased with the progression of the reaction, resulting from the further dehydration of xylose in solution, generating FF and other by-products. Wang

Table 2. Pore structure of the fresh, used and regenerated catalysts

Catalysts	Pore volume (cm^3/g)	Surface area (m^2/g)	Average pore size (nm)	Most probable pore size (nm)
01	0.038	13.8	32.0	62.9
07	0.027	3.2	29.8	47.3
08	0.036	11.5	31.5	59.6
14	0.021	2.5	28.4	46.4
15	0.037	12.5	30.3	60.2
21	0.025	3.3	27.4	42.2
22	0.032	11.3	29.9	62.4
28	0.019	2.0	26.3	43.1

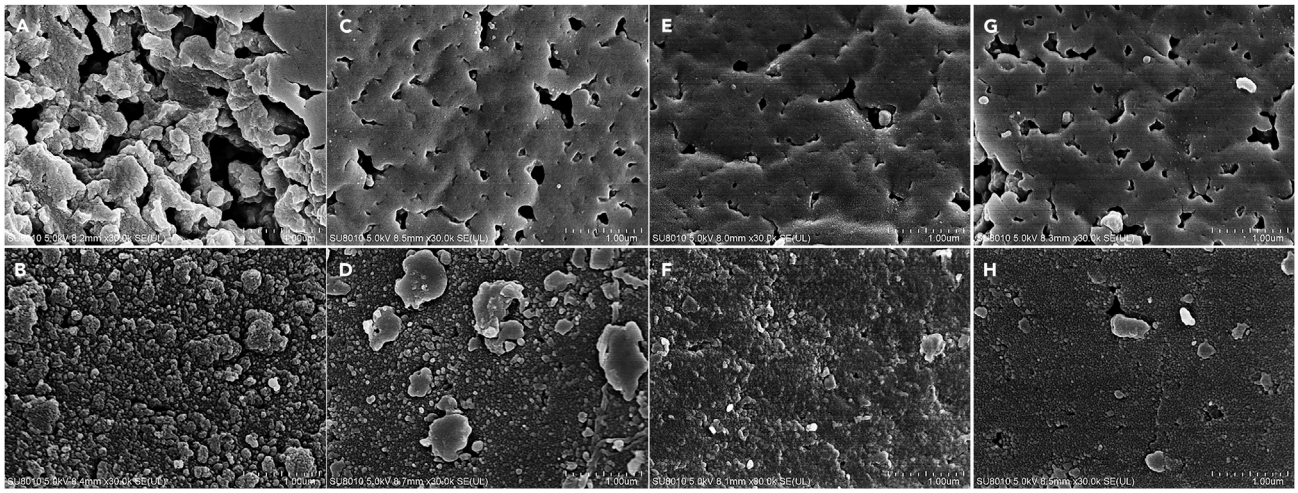

Figure 3. SEM images of fresh, used and regenerated catalysts

(A) Fresh catalyst.
(B) Used catalyst numbered 07.
(C) Regenerated catalyst numbered 08.
(D) Used catalyst numbered 14.
(E) Regenerated catalyst numbered 15.
(F) Used catalyst numbered 21.
(G) Regenerated catalyst numbered 22.
(H) Used catalyst numbered 28.

et al.[29] investigated the conversion of different xylan-type hemicelluloses to xylose and FF in a two-phase system using $SnCl_4$ as the catalyst and 2-methyltetrahydrofuran/H_2O as solvent. They found that the yield of FF and xylose was related to the content, molecular weight, and crystallinity of hemicellulose in biomass. The hemicellulose in the corn stover used in this study has a typical xylan-type hemicellulose structure with low molecular weight and crystallinity, and the corn stover has low lignocellulose recalcitrance.[3] Consequently, it is easy to hydrolyze to xylose and further dehydrate to FF under milder conditions. The highest xylose yield was 91.3 mol %, achieved after 40 min reaction at 130°C

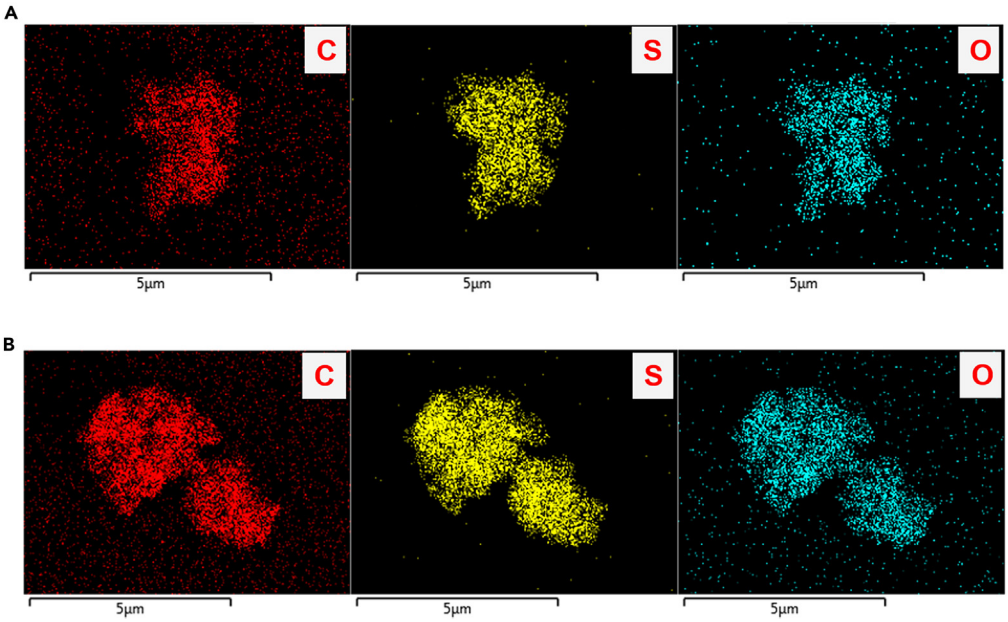

Figure 4. EDS analysis of fresh and used catalysts

(A) Fresh catalyst.
(B) Used catalyst after 28 catalytic runs.

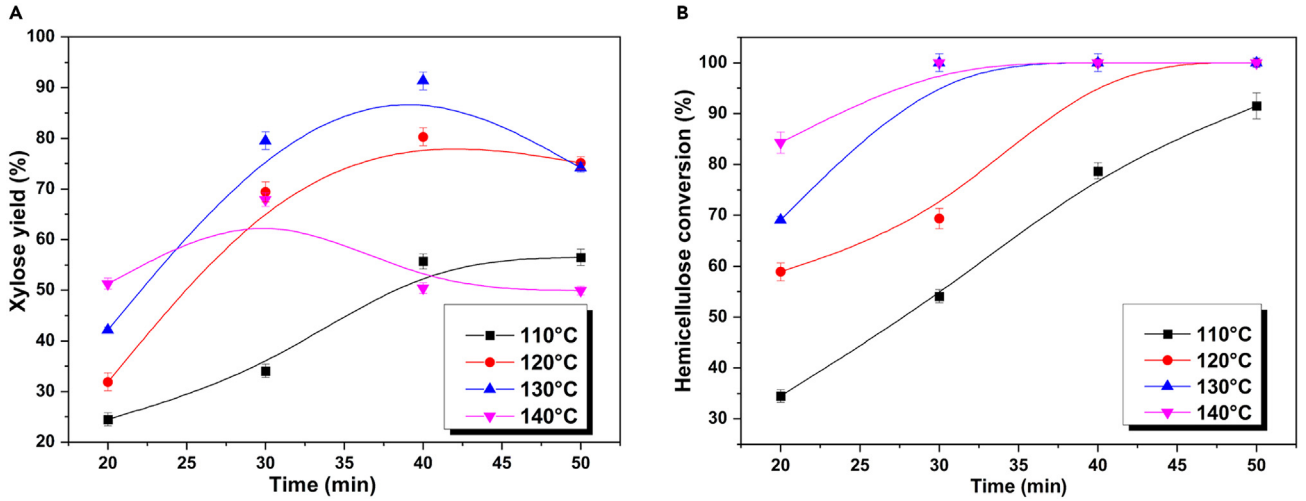

Figure 5. Hydrolysis of corn stover to xylose-rich hydrolysate

20 g corn stover, 300 mL 0.9 wt. % sulfuric acid solution.

(A) Xylose yield.

(B) Hemicellulose conversion.

(based on hemicellulose). The hemicellulose conversion was 100%, indicating that the dilute acid hydrolysis process could completely release the xylose units from biomass. However, under these conditions, FF was not detected in the products, indicating that besides xylose, hemicellulose was primarily converted to other soluble sugars, such as arabinose, xylan, glucose, and mannose, along with some FF precursor compounds.

Second step hydrolysis for the conversion of cellulose to glucose

The cellulose-containing residue obtained after primary hydrolysis was further hydrolyzed at higher temperatures to release the glucose units from the biomass. The results are shown in Figure 6. Compared with hemicellulose, cellulose has a more closely connected structure, and its hydrolysis requires higher chemical energy.[30] Thus, higher temperatures are necessary for the complete hydrolysis of cellulose. The trend in the variation of glucose yields was similar to that of xylose yields at the same temperature. Prolonged reaction time is harmful to glucose retention due to further isomerization and dehydration of the generated glucose to HMF in the acid-catalyzed system, as well as the additional

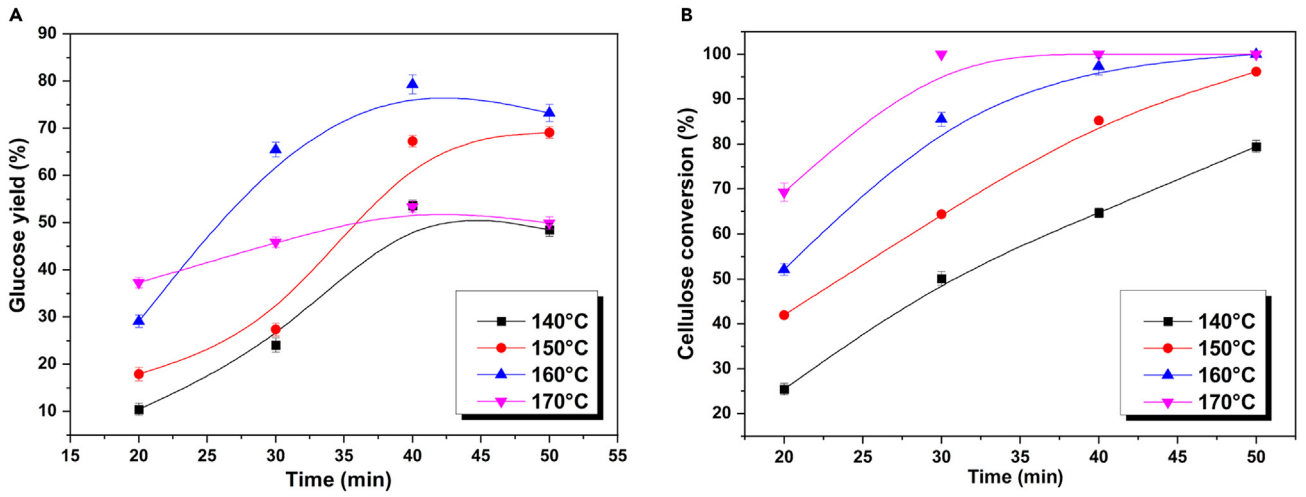

Figure 6. Hydrolysis of cellulose-containing residue to glucose-rich hydrolysate

20 g of cellulose-containing residue from primary hydrolysis, 300 mL 0.9 wt. % sulfuric acid solution.

(A) Glucose yield.

(B) Cellulose conversion.

hydration of HMF to LA. Morales et al.[31] conducted a study on acid hydrolysis with a pure aqueous solvent for glucose production from cellulose. It was found that appropriate reaction temperatures and lower acid concentrations resulted in high glucose yields while reducing the formation of LA. Hydrolysis at 160°C for 40 min yielded up to 79.3 mol % glucose (based on the molar yield of cellulose) and 97.3% cellulose conversion. The hydrolysis products did not contain HMF and LA, indicating that cellulose was mainly converted to glucose as well as other soluble saccharides under this condition.

Conversion of hydrolysate to FF and LA

After two-step hydrolysis with dilute acid, the hydrolysate rich in xylose or glucose was obtained. Based on the aforementioned hydrolyzed sugar solution, the hydrothermal conversion of the hydrolysate was carried out using the prepared resin solid acid as catalyst, and the mass yields of FF and LA obtained based on the dry biomass are shown in Figure 7. In a pure water system, with 60 min solid acid catalysis of hydrolysate at 170°C, the mass yield of FF was up to 12.6 wt. %. This result corresponds to a FF molar yield of 68.7 mol % based on hemicellulose, which is significantly higher than those obtained in previous studies using single homogeneous or solid acid (generally below 50 mol %). The results of FTIR and the SACs of catalysts indicate that the solid acid provided abundant strong acid sites (-SO_3H). In addition, it promoted the isomerization of xylose to xylulose through the weak acid site on its phenolic hydroxyl group.

Additionally, the pure water system proved to be more favorable for LA production, resulting in a maximum LA mass yield of up to 14.7 wt. % at 200°C, equivalent to a molar yield of 70.3 mol % based on cellulose. The total mass yields of FF and LA, based on dry biomass, reached 27.3 wt. %, a significant improvement compared to previous studies.[19,32–34] For example, Galletti et al.[35] tested LA production from various biomass (poplar sawdust, paper mill sludge, tobacco chips, wheat straws, and olive branches), where the highest LA yield of 59 mol % was obtained, corresponding to LA yield of 25 wt. % based on cellulose in the feedstock, in the presence of HCl/H_2SO_4 catalyst. Notably, this catalytic system can convert both hemicellulose and cellulose efficiently and directionally, enabling the conversion of various lignocellulosic biomass into FF and LA in the same catalytic system. The mass yield of FF and LA for barley straw, rice straw, sorghum straw, lauan, and pinus sylvestris were 29.3%, 25.6%, 25.2%, 28.4%, and 23.6%, respectively.

The comparison between this study and other relevant studies is shown in Table 3. In this study, by integrating H_2SO_4-assisted hydrothermal hydrolysis with solid acid catalytic conversion, corn stover can be efficiently hydrothermal decomposed and converted into FF and LA in a shorter reaction time.

Recycling performance

To have an insight into the stability of resin-based solid acid catalyst, a recycling performance evaluation was conducted for 28 catalytic runs. Catalyst regeneration was performed after every 7 catalytic runs, which was defined as a reaction period. As shown in Figure 8, the initial FF yields for each reaction period were 68.7 mol %, 70.2 mol %, 69.1 mol %, and 65.5 mol %, respectively. Meanwhile, at the end of each reaction period, the corresponding FF yields were 55.1 mol %, 52.4 mol %, 54.5 mol %, and 51.4 mol %. These results indicated that the catalytic activity of the catalyst can be quickly restored to the initial state by introducing a simple catalyst regeneration step, thus, the catalyst recycling performance can be enhanced effectively.

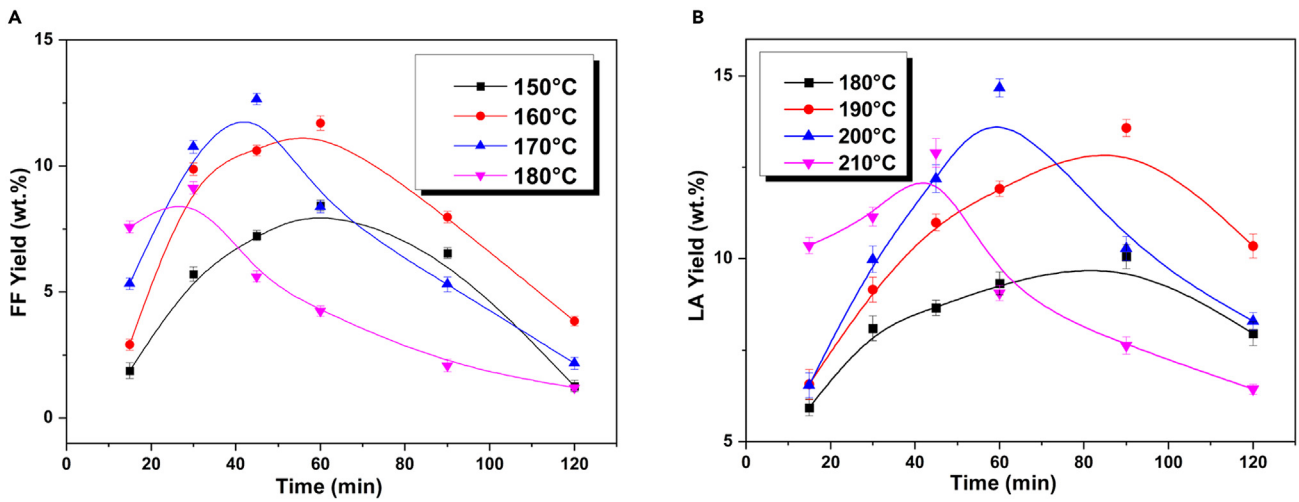

Figure 7. Hydrolysate to FF and LA catalyzed by solid acid catalyst

300 mL hydrolysate, 3 g catalyst, mass yield based on dry substrate biomass.

(A) Mass yield of FF.

(B) Mass yield of LA.

Table 3. Comparison of this study with previous reports from other laboratories

Raw materials	Catalyst	Reaction conditions	Solvents	Conversion (mol %)	[c] X/[d] G yield (mol %)	FF/LA yield (mol %)	Reference
Poplar	$[MIMPS]_2H_4P_2Mo_{18}$	150°C-170°C, 12–14 h,	Ionic liquid	[a] H 90.4, [b] C 100	[c] X 12.9, [d] G 32.9	–	Li et al.[36]
Corn straw	$(CTA)H_2PW$	150°C, 12 h,	Water	–	[c] X 8.3, [d] G 19.8	–	Song et al.[37]
Cellobiose	$[HO_3S-(CH_2)_3-mim]Cl-FeCl_3$	180°C, 10 h	Water	–	—, [d] G 10.9	LA 67.5	Liu et al.[38]
Glucose	Cation exchange resin	145°C, 24 h	Water	100	–	LA 70.7	Pyo et al.[39]
Xylose	LC-1S	175°C, 3 h	Water-MIBK	96.7	–	FF 64.8	Antonyraj et al.[40]
Xylose	Glu-TsOH-Ti	180°C, 30 min	Water-THF	–	–	FF 51	Mazzotta et al.[41]
Corn stover	0.9 wt. % H_2SO_4	130°C-160°C, 40 min,	Water	[a] H 100, [b] C 97.3	[c] X 91.3, [d] G 79.3	–	This work
Corn stover hydrolysate	Resin solid acid	170°C-200°C, 60 min	Water	–	–	FF 68.7, LA 70.3	This work

[a]H refers to the hemicellulose.
[b]C refers to the cellulose.
[c]X refers to the xylose.
[d]G refers to the glucose.

A similar change pattern was observed in the systematic characterization of the fresh and used catalysts, including SAC, sulfur content, and pore structure. With the increase in cycling times, both SAC and sulfur content gradually decreased. Simultaneously, pore size and specific surface area also decreased continuously due to the enrichment of humins. It can be seen from Figure 8 that compared with the FF yield, the cycling process had a relatively minor impact on LA yield. In the first reaction period, the yield of LA decreased from 71.5 mol % to 63.1 mol %, and in the fourth reaction period, it decreased from 68.4 mol % to 59.5 mol %. After four reaction periods, catalyst performance reduced to 83% of the initial catalytic performance in the conversion of glucose to LA. The conversion of xylose and glucose was maintained at the initial level, exceeding 99%.

In the dilute sulfuric acid/solid acid catalysis system, sulfuric acid and solid acid demonstrated a synergistic catalytic effect. It is known that xylose in the hydrolysate would be isomerized into xylulose through hydrogen transfers from O2 to O1 and C2 to C1 separately, and was then dehydrated to produce FF.[42] In this process, the conjugated base provided by diluted sulfuric acid and the weak acid site on the solid acid facilitated the 1,2-hydrogen transfer, while H^+ and the strong acid sites on the solid acid played a dominant role in the subsequent dehydration process. For the hydrolysate containing glucose, under the synergistic catalysis of dilute acid and solid acid, glucose was isomerized to

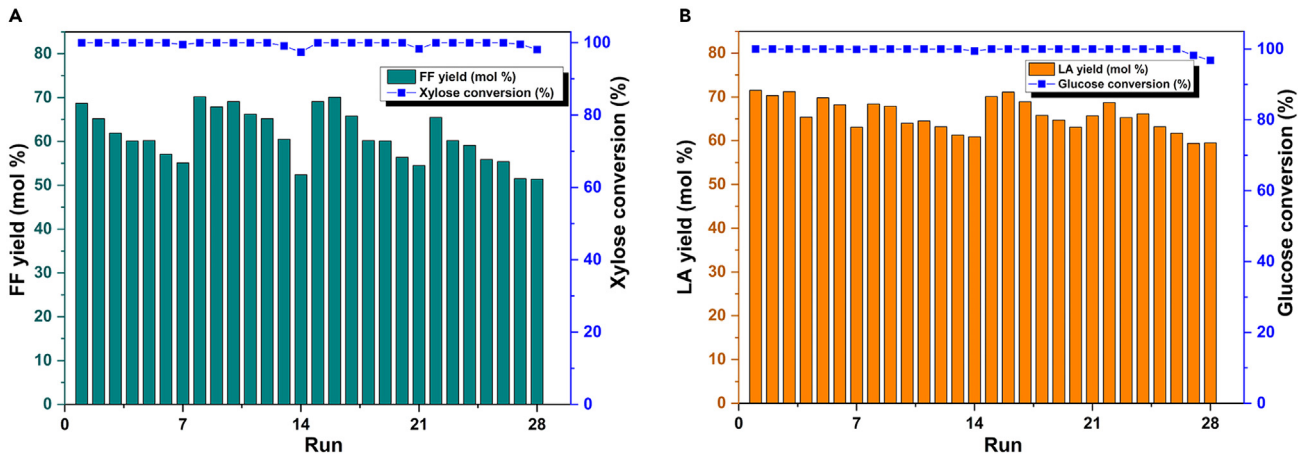

Figure 8. Recovery performance evaluation of solid acid catalyst during 28 catalytic runs
300 mL hydrolysate, 3 g catalyst, 170°C/45 min for xylose hydrothermal conversion, 200°C/60 min for glucose hydrothermal conversion.
(A) Molar yield of FF.
(B) Molar yield of LA.

fructose which was similar to the isomerization of xylose. And then fructose was protonated and dehydrated to form fructosyl carbonium ions (five-membered carbonium ion), which were further deprotonated to form two intermediates, frutofuranosyl and 2,6-anhydro-β-D-fructofuranose.[43,44] Among them, intermediate of frutofuranosyl could generate HMF through two-step dehydration, while 2,6-anhydro-β-D-fructofuranose was more likely to promote the formation of humins. Interestingly, the weak acid sites on the solid acid could promote the formation of the intermediate of frutofuranosyl,[45] thereby reducing the probability of the process generating humins. Furthermore, under the catalysis of strong acid sites of dilute acid and solid acid, water is added to the furan ring C2-C3 bonds of HMF to form LA and formic acid as final products.[46]

Conclusions

This study synthesized a novel resin-derived carbon-based solid acid catalyst with large pores and developed a two-stage hydrothermal conversion process, namely dilute acid hydrolysis coupled with solid acid catalytic conversion process, for the efficient conversion of lignocellulose biomass to the precursors of aviation fuel, FF and LA. The catalyst has a uniform distribution of active functional groups, high catalytic activity, and high hydrothermal stability. Its SAC is up to 2.63 mmol/g, and there is only slight deactivation during the four reaction periods. The catalyst demonstrates a typical characteristic peak of sulfonic acid group (-SO_3H) as shown by analysis of FTIR. The recycling process has little impact on the main structure of the catalyst. The decline in catalyst performance was mainly due to the continuous enrichment of humins on the catalyst during the recycling process, which was confirmed by SEM, TEM, and pore structure analysis. However, a simple catalytic activation and regeneration process could effectively remove humins and restore the catalytic activity. After 28 catalytic runs, the catalyst retains 83% of the initial catalytic performance. The conversions of hemicellulose and cellulose in corn stover were 100% and 97.3%, respectively, under this catalytic conversion process. The FF and LA yields were 68.7 mol % and 70.3 mol %, respectively. Additionally, the total mass yield of FF and LA was 27.3 wt. %.

Limitations of the study

The limitations of this study include two issues. Firstly, the multi-step hydrothermal conversion process in the current experiment requires manual separation, and we are conducting continuous automated experimental research; Secondly, the lifetime of the catalyst is relatively good among similar catalysts, but it is still necessary to carry out research to improve the stability of the catalyst and make it suitable for practical application.

STAR★METHODS

Detailed methods are provided in the online version of this paper and include the following:

- KEY RESOURCES TABLE
- RESOURCE AVAILABILITY
  - Lead contact
  - Materials availability
  - Data and code availability
- METHOD DETAILS
  - Raw material analysis
  - Catalyst preparation
  - Hydrothermal conversion of biomass
  - Catalyst characterization
- QUANTIFICATION AND STATISTICAL ANALYSIS

SUPPLEMENTAL INFORMATION

Supplemental information can be found online at https://doi.org/10.1016/j.isci.2023.108249.

ACKNOWLEDGMENTS

This research is supported by the National Key Research and Development Program of China (No.2018YFB1501500) and the National Science Fund for Distinguished Young Scholars (No. 51725603).

AUTHOR CONTRIBUTIONS

Conceptualization, L.Z. and S.W.; Methodology, L.Z. and H.X.; Formal Analysis, L.Z. and H.X.; Investigation, L.Z. and H.X.; Writing – Original Draft, L.Z. and H.X.; Writing – Review & Editing, L.Z. and X.Y.; Visualization, L.Z. and X.Y.; Supervision, S.W.; Funding Acquisition, S.W.

DECLARATION OF INTERESTS

The authors declare no competing interests.

Received: May 15, 2023
Revised: August 2, 2023
Accepted: October 16, 2023
Published: October 18, 2023

REFERENCES

1. Wang, Y., Liu, P., Zhang, G., Yang, Q., Lu, J., Xia, T., Peng, L., and Wang, Y. (2021). Cascading of engineered bioenergy plants and fungi sustainable for low-cost bioethanol and high-value biomaterials under green-like biomass processing. Renew. Sustain. Energy Rev. *137*, 110586. https://doi.org/10.1016/j.rser.2020.110586.
2. Zhang, R., Gao, H., Wang, Y., He, B., Lu, J., Zhu, W., Peng, L., and Wang, Y. (2023). Challenges and perspectives of green-like lignocellulose pretreatments selectable for low-cost biofuels and high-value bioproduction. Bioresour. Technol. *369*, 128315. https://doi.org/10.1016/j.biortech.2022.128315.
3. Wu, L., Feng, S., Deng, J., Yu, B., Wang, Y., He, B., Peng, H., Li, Q., Hu, R., and Peng, L. (2019). Altered carbon assimilation and cellulose accessibility to maximize bioethanol yield under low-cost biomass processing in corn brittle stalk. Green Chem. *21*, 4388–4399. https://doi.org/10.1039/c9gc01237k.
4. Zhao, Y., Lu, K., Xu, H., Zhu, L., and Wang, S. (2021). A critical review of recent advances in the production of furfural and 5-hydroxymethylfurfural from lignocellulosic biomass through homogeneous catalytic hydrothermal conversion. Renew. Sustain. Energy Rev. *139*, 110706. https://doi.org/10.1016/j.rser.2021.110706.
5. Xiong, S., Guan, Y., Luo, C., Zhu, L., and Wang, S. (2021). Critical review on the preparation of platform compounds from biomass or saccharides via hydrothermal conversion over carbon-based solid acid catalysts. Energy Fuels *35*, 14462–14483. https://doi.org/10.1021/acs.energyfuels.1c02672.
6. Hoydonckx, H.E., Van Rhijn, W.M., Van Rhijn, W., De Vos, D.E., and Jacobs, P.A. (2007). Furfural and derivatives. Ullmann's Encycl. Ind. Chem. *16*, 285–313. https://doi.org/10.1002/14356007.a12_119.pub2.
7. Ramli, N.A.S., and Amin, N.A.S. (2016). Optimization of biomass conversion to levulinic acid in acidic ionic liquid and upgrading of levulinic acid to ethyl levulinate. Bioenergy Res. *10*, 50–63. https://doi.org/10.1007/s12155-016-9778-3.
8. Zhou, C., Yu, X., Ma, H., He, R., and Vittayapadung, S. (2013). Optimization on the conversion of bamboo shoot shell to levulinic acid with environmentally benign acidic ionic liquid and response surface analysis. Chin. J. Chem. Eng. *21*, 544–550. https://doi.org/10.1016/S1004-9541(13)60509-1.
9. Novodárszki, G., Rétfalvi, N., Dibó, G., Mizsey, P., Cséfalvay, E., and Mika, L.T. (2014). Production of platform molecules from sweet sorghum. RSC Adv. *4*, 2081–2088. https://doi.org/10.1039/c3ra42895h.
10. Zhao, Y., Lu, K., Xu, H., Qu, Y., Zhu, L., and Wang, S. (2019). Comparative study on the dehydration of biomass-derived disaccharides and polysaccharides to 5-Hydroxymethylfurfural. Energy Fuels *33*, 9985–9995. https://doi.org/10.1021/acs.energyfuels.9b02863.
11. Zhao, Y., Xu, H., Lu, K., Qu, Y., Zhu, L., and Wang, S. (2019). Experimental and kinetic study of arabinose conversion to furfural in renewable butanone-water solvent mixture catalyzed by lewis acidic ionic liquid catalyst. Ind. Eng. Chem. Res. *58*, 17088–17097. https://doi.org/10.1021/acs.iecr.9b03420.
12. Zhao, Y., Xu, H., Lu, K., Qu, Y., Zhu, L., and Wang, S. (2019). Dehydration of xylose to furfural in butanone catalyzed by Brønsted-Lewis acidic ionic liquids. Energy Sci. Eng. *7*, 2237–2246. https://doi.org/10.1002/ese3.444.
13. Zhao, Y., Xu, H., Wang, K., Lu, K., Qu, Y., Zhu, L., and Wang, S. (2019). Enhanced furfural production from biomass and its derived carbohydrates in the renewable butanone-water solvent system. Sustain. Energy Fuels *3*, 3208–3218. https://doi.org/10.1039/c9se00459a.
14. Xiong, K., and Chen, J.G. (2020). Correlating furfural reaction pathways with interactions between furfural and monometallic surfaces. Catal. Today *339*, 289–295. https://doi.org/10.1016/j.cattod.2018.10.004.
15. Li, H., Ren, J., Zhong, L., Sun, R., and Liang, L. (2015). Production of furfural from xylose, water-insoluble hemicelluloses and water-soluble fraction of corncob via a tin-loaded montmorillonite solid acid catalyst. Bioresour. Technol. *176*, 242–248. https://doi.org/10.1016/j.biortech.2014.11.044.
16. Gupta, N.K., Fukuoka, A., and Nakajima, K. (2017). Amorphous Nb_2O_5 as a selective and reusable catalyst for furfural production from xylose in biphasic water and toluene. ACS Catal. *7*, 2430–2436. https://doi.org/10.1021/acscatal.6b03682.
17. Li, X., Lu, X., Hu, W., Xu, H., Chen, J., Xiong, J., Lu, L., Yu, Z., and Si, C. (2022). Phosphotungstic acid functionalized biochar for furfural production from corncob. Fuel Process. Technol. *229*, 107178. https://doi.org/10.1016/j.fuproc.2022.107178.
18. Wang, Y., Delbecq, F., Kwapinski, W., and Len, C. (2017). Application of sulfonated carbon-based catalyst for the furfural production from D-xylose and xylan in a microwave-assisted biphasic reaction. Mol. Catal. *438*, 167–172. https://doi.org/10.1016/j.mcat.2017.05.031.
19. Shen, Z., Yu, X., and Chen, J. (2016). Production of 5-hydroxymethylfurfural from fructose catalyzed by sulfonated bamboo-derived carbon prepared by simultaneous carbonization and sulfonation. Bioresources *11*, 3094–3109. https://doi.org/10.15376/biores.11.2.3094-3109.
20. Gan, L., Zhu, J., and Lv, L. (2017). Cellulose hydrolysis catalyzed by highly acidic lignin-derived carbonaceous catalyst synthesized via hydrothermal carbonization. Cellulose *24*, 5327–5339. https://doi.org/10.1007/s10570-017-1515-3.
21. Zhu, Y., Li, W., Lu, Y., Zhang, T., Jameel, H., Chang, H.M., and Ma, L. (2017). Production of furfural from xylose and corn stover catalyzed by a novel porous carbon solid acid in γ-valerolactone. RSC Adv. *7*, 29916–29924. https://doi.org/10.1039/c7ra03995f.
22. Zhang, T., Li, W., An, S., Huang, F., Li, X., Liu, J., Pei, G., and Liu, Q. (2018). Efficient transformation of corn stover to furfural using p-hydroxybenzenesulfonic acid-formaldehyde resin solid acid. Bioresour. Technol. *264*, 261–267. https://doi.org/10.1016/j.biortech.2018.05.081.
23. Xiong, S., Luo, C., Yu, Z., Ji, N., Zhu, L., and Wang, S. (2021). Dual -functional carbon-based solid acid-induced hydrothermal conversion of biomass saccharides: Catalyst rational design and kinetic analysis. Green Chem. *23*, 8458–8467. https://doi.org/10.1039/d1gc01968f.
24. Wang, S., Luo, C., Zhao, Y., Chen, J., and Zhou, J. (2016). Structural characterization and pyrolysis behavior of humin by-products from the acid-catalyzed conversion of C6 and C5 carbohydrates. Methods Mol. Biol. *1342*, 259–268. https://doi.org/10.1016/j.jaap.2016.02.009.
25. Geng, L., Wang, Y., Yu, G., and Zhu, Y. (2011). Efficient carbon-based solid acid catalysts for the esterification of oleic acid. Catal. Commun. *13*, 26–30. https://doi.org/10.1016/j.catcom.2011.06.014.
26. Ballotin, F.C., Da Silva, M.J., Lago, R.M., and Teixeira, A.P.d.C. (2020). Solid acid catalysts based on sulfonated carbon nanostructures embedded in an amorphous matrix produced from bio-oil: Esterification of oleic acid with methanol. J. Environ. Chem. Eng. *8*, 103674. https://doi.org/10.1016/j.jece.2020.103674.
27. Cao, M., Peng, L., Xie, Q., Xing, K., Lu, M., and Ji, J. (2021). Sulfonated Sargassum horneri carbon as solid acid catalyst to produce biodiesel via esterification. Bioresour. Technol. *324*, 124614. https://doi.org/10.1016/j.biortech.2020.124614.
28. Cheng, Z., Everhart, J.L., Tsilomelekis, G., Nikolakis, V., Saha, B., and Vlachos, D.G. (2018). Structural analysis of humins formed in the Brønsted acid catalyzed dehydration of fructose. Green Chem. *20*, 997–1006. https://doi.org/10.1039/c7gc03054a.
29. Wang, W., Ren, J., Li, H., Deng, A., and Sun, R. (2015). Direct transformation of xylan-type hemicelluloses to furfural via $SnCl_4$ catalysts in aqueous and biphasic systems. Bioresour. Technol. *183*, 188–194. https://doi.org/10.1016/j.biortech.2015.02.068.
30. Wang, S., Dai, G., Yang, H., and Luo, Z. (2017). Lignocellulosic biomass pyrolysis mechanism: A state-of-the-art review. Prog. Energy Combust. Sci. *62*, 33–86. https://doi.org/10.1016/j.pecs.2017.05.004.
31. Morales-delaRosa, S., Campos-Martin, J.M., and Fierro, J.L.G. (2014). Optimization of the process of chemical hydrolysis of cellulose to glucose. Cellulose *21*, 2397–2407. https://doi.org/10.1007/s10570-014-0280-9.
32. Liu, Y., Wang, C., Chen, M., Zhao, W., Yang, T., and Yang, S. (2017). Catalytic conversion of carbohydrates to levulinic acid with mesoporous niobium-containing oxides.

J. Environ. Sci. *55*, 20–32. https://doi.org/10.1016/j.catcom.2017.01.023.

33. Tukacs, J.M., Holló, A.T., Rétfalvi, N., Cséfalvay, E., Dibó, G., Havasi, D., and Mika, L.T. (2017). Microwave-assisted valorization of biowastes to levulinic acid. ChemistrySelect *2*, 1375–1380. https://doi.org/10.1002/slct.201700037.
34. Thombal, P.R., and Han, S.S. (2018). Novel synthesis of Lewis and Bronsted acid sites incorporated CS-Fe_3O_4@SO_3H catalyst and its application in one-pot synthesis of tri(furyl) methane under aqueous media. Biofuel Res. J. *5*, 886–893. https://doi.org/10.18331/BRJ2018.5.4.3.
35. Galletti, A.M.R., Antonetti, C., De Luise, V., Licursi, D., and Nassi o Di Nasso, N. (2012). Levulinic acid production from waste biomass. Bioresources *7*, 1824–1835. https://doi.org/10.1007/s40664-017-0218-9.
36. Li, Y., Zhang, X., Li, Z., Song, J., and Wang, X. (2019). Full utilization of lignocellulose with ionic liquid polyoxometalates in a one-pot three-step conversion. ChemSusChem *12*, 4936–4945. https://doi.org/10.1002/cssc.201902503.
37. Song, J., Li, Y., Zhang, X., Zhang, D., Jiang, Z., and Wang, X. (2019). Mesoporous heteropolyacid nanorods for heterogeneous catalysis in polysaccharide conversion. Bioresources *15*, 240–264. https://doi.org/10.15376/biores.15.1.240-264.
38. Liu, S., Wang, K., Yu, H., Li, B., and Yu, S. (2019). Catalytic preparation of levulinic acid from cellobiose via Brønsted-Lewis acidic ionic liquids functional catalysts. Sci. Rep. *9*, 1810. https://doi.org/10.1038/s41598-018-38051-y.
39. Pyo, S.H., Glaser, S.J., Rehnberg, N., and Hatti-Kaul, R. (2020). Clean production of levulinic acid from fructose and glucose in salt water by heterogeneous catalytic dehydration. ACS Omega *5*, 14275–14282. https://doi.org/10.1021/acsomega.9b04406.
40. Antonyraj, C.A., and Haridas, A. (2018). A lignin-derived sulphated carbon for acid catalyzed transformations of bio-derived sugars. Catal. Commun. *104*, 101–105. https://doi.org/10.1016/j.catcom.2017.10.029.
41. Mazzotta, M.G., Gupta, D., Saha, B., Patra, A.K., Bhaumik, A., and Abu-Omar, M.M. (2014). Efficient solid acid catalyst containing Lewis and Brønsted acid sites for the production of furfurals. ChemSusChem *7*, 2342–2350. https://doi.org/10.1002/cssc.201402007.
42. Choudhary, V., Sandler, S.I., and Vlachos, D.G. (2012). Conversion of xylose to furfural using Lewis and Brønsted acid catalysts in aqueous media. ACS Catal. *2*, 2022–2028. https://doi.org/10.1021/cs300265d.
43. Van Putten, R.J., Van Der Waal, J.C., De Jong, E., Rasrendra, C.B., Heeres, H.J., and De Vries, J.G. (2013). Hydroxymethylfurfural, a versatile platform chemical made from renewable resources. Chem. Rev. *113*, 1499–1597. https://doi.org/10.1021/cr300182k.
44. Akien, G.R., Qi, L., and Horváth, I.T. (2012). Molecular mapping of the acid catalysed dehydration of fructose. Chem. Commun. *48*, 5850–5852. https://doi.org/10.1039/c2cc31689g.
45. Yang, G., Pidko, E.A., and Hensen, E.J. (2012). Mechanism of Brønsted acid-catalyzed conversion of carbohydrates. J. Catal. *295*, 122–132. https://doi.org/10.1016/j.jcat.2012.08.002.
46. Zhang, J.H., Yang, R., Wang, T.Y., Dong, W.H., Wang, F., and Wang, L. (2012). An in situ NMR study of the mechanism for the catalytic conversion of fructose to 5-Hydroxymethylfurfural and then to levulinic acid using ^{13}C labeled D-fructose. ACS Catal. *6*, 1211–1213. https://doi.org/10.1021/cs300045r.
47. Li, Z., Yang, J., Zhao, J., Han, P., Chai, Z., and Feng, Y. (2016). Effect of extractives on digestibility of cellulose in corn stover with liquid hot water pretreatment. Bioresources *16*, 54–70. https://doi.org/10.15376/biores.11.1.54-70.
48. Li, D., Wang, Q., Li, J., Li, Z., Yuan, Y., Yan, Z., Mei, Z., and Liu, X. (2016). Mesophilic-hydrothermal-thermophilic (M-H-T) digestion of green corn straw. Bioresour. Technol. *202*, 25–32. https://doi.org/10.1016/j.biortech.2015.11.073.
49. Biermann, C.J., and McGinnis, G.D. (1989). Analysis of Carbohydrates by GLC and MS (CRC Press), pp. 255–256.
50. Selvendran, R.R., March, J.F., and Ring, S.G. (1979). Determination of aldoses and uronic acid content of vegetable fiber. Anal. Biochem. *96*, 282–292. https://doi.org/10.1016/0003-2697(79)90583-9.

STAR★METHODS

KEY RESOURCES TABLE

REAGENT or RESOURCE	SOURCE	IDENTIFIER
Chemicals, peptides, and recombinant proteins		
Chitosan	Sinopharm Group Chemical Reagent Co., Ltd.	CAS: 9012-76-4
Sulfuric acid	Sinopharm Group Chemical Reagent Co., Ltd.	CAS: 7664-93-9
p-hydroxybenzenesulfonic acid	Shanghai Aladdin Biochemical Technology Co., Ltd.	CAS: 98-67-9
Formaldehyde	Sinopharm Group Chemical Reagent Co., Ltd.	CAS: 50-00-0
Acetic acid	Shanghai Aladdin Biochemical Technology Co., Ltd.	CAS: 64-19-7
Glucose	Shanghai Macklin Biochemical Co., Ltd.	CAS: 50-99-7
D-Xylose	Shanghai Macklin Biochemical Co., Ltd.	CAS: 6763-34-4
Furfural	Shanghai Macklin Biochemical Co., Ltd.	CAS: 98-01-1
Levulinic acid	Shanghai Macklin Biochemical Co., Ltd.	CAS: 123-76-2
Corn stover	Liaoning Changyuan straw processing plant	

RESOURCE AVAILABILITY

Lead contact

Further information and requests for resources and reagents should be directed to and will be fulfilled by the lead contact, Shurong Wang (srwang@zju.edu.cn).

Materials availability

This study did not generate new unique reagents.

Data and code availability

- All data reported in this paper will be shared by the lead contact upon request.
- This paper does not report original code.
- Any additional information required to reanalyze the data reported in this paper is available from the lead contact upon request.

METHOD DETAILS

Raw material analysis

The components distribution and element composition of corn stover were analyzed (further details in the supporting information, Table S1). Among them, the extracts mainly include soluble sugars, phenols, lipids and waxes.[47] The content of soluble sugars in corn straw of 8.13% was reported by Li et al.[48] And some wide type of corn stalk was reported having16.42% of soluble sugars, while for some selected corn stalk the value can reach to 27.25%, which was much higher than that of other grassy crops.[3] The corn stalk with higher soluble sugars were directly convertible and fermentable, leading to have a high bioethanol yield.

Catalyst preparation

For the research, 1 g of chitosan was added to 50 mL of distilled water at a temperature of 60°C and magnetic stirring was initiated. When the chitosan was completely dissolved, 6 g of PHSA was added and mixed thoroughly until the solution became clear. Next, 10 mL of FF (99.5 wt. %) and 1 mL of formaldehyde solution (10 wt. %) were added simultaneously. In this mixture, FF reacted with PHSA via a condensation reaction, with formaldehyde acting as the reaction promoter. Magnetic stirring was continued for another 10 min, and an ultrasonic generator was used to eliminate any air bubbles that may have formed during the reaction. Next, 10 mL of acetic acid (50 wt. %) was dropwise added to the previously prepared mixture as a curing agent, and the solid was dried in an oven at 105°C for 12 h, yielding the resinous solid acid catalyst. The catalyst was pelletized into small spherical particles of diameter 1 mm using a granulator for research. The schematic diagram of catalyst skeleton formation is illustrated in Figure S1.

Hydrothermal conversion of biomass

The biomass was converted through hydrothermal methods in two stages. The process scheme was shown in Figure S2. Firstly, xylose/glucose solutions were obtained by hydrolyzing biomass with a dilute sulfuric acid. Subsequently, sugar solutions were converted to produce FF and LA using a resinous solid acid as a catalyst. The detailed experimental process is described as follows: 20 g fully dried corn stover powder with

60–80 mesh mixed with 300 mL sulfuric acid solution (0.9 wt. %), and was subjected to primary hydrolysis at 110°C–140°C for 20-50 min to obtain a xylose-containing solution. Cellulose-containing solid residue was separated and hydrolyzed again in 300 mL sulfuric acid solution (0.9 wt. %) at 140°C-170°C to obtain a glucose-containing solution. For solid acid catalysis, 300 mL sugar solution was added to a 500 mL tank reactor, along with 3 g carbon-based solid acid catalyst. The reaction was carried out for 15–120 min at 150°C–210°C. The resulting liquid phase product was diluted ten times with deionized water and analyzed to determine the product composition. The UltiMate 3000 (Thermo Scientific) high-performance liquid chromatography equipped with Bio-rad HPX-87H (7.8 mm × 300 mm) column and RI2000 differential refractive index detector (Schambeck SFD) was used to quantify the main raw materials and products, such as xylose, glucose, fructose, FF, and LA. The mobile phase was a 0.005 mol/L sulfuric acid solution with a flow rate of 0.6 mL/min. The hemicellulose and cellulose conversions were determined using the so-called SAEMAN method by subjecting the hydrolysis residue to further hydrolysis under specific conditions. The xylose and glucose obtained after hydrolysis were classified into unconverted hemicellulose and cellulose in biomass.[49,50] In order to improve the cycling performance of the solid acid catalysts, 7 catalytic runs were taken as a reaction period. After each reaction period, the catalysts were treated for regeneration. The regeneration process involved ultrasonic cleaning of the catalysts at 50°C using deionized water and acetone as solvents, followed by sulfonation in 70 wt. % concentrated sulfuric acid for 30 min at ambient temperature. The fresh catalyst and regeneration catalysts were numbered 01, 08, 15 and 22, while the catalysts after each reaction period were numbered 07, 14, 21 and 28, respectively.

Catalyst characterization

The catalysts used during different reaction periods were systematically characterized. The stability of the catalysts was evaluated through thermogravimetric (TG) analysis, which was carried out on an STA 409 PC/PG simultaneous thermal analyzer. The test was performed under a nitrogen flow of 30 mL/min, and the temperature was increased from 30°C to 800°C at a rate of 10°C/min. The functional group information of the catalysts was analyzed using a Nicolet 5700 FTIR spectrometer. The contents of C, H, O, N, and S elements were determined using a Vario Macro Elementer. The specific surface area and pore size distribution of the catalysts were investigated on a specific surface and pore size analyzer (AUTOSORB-IQ2-MP). The surface morphology of the catalysts was analyzed using a field-emission scanning electron microscope (SEM). Energy-dispersive X-ray spectroscopy (EDS) analysis was also carried out to obtain the dispersion of C, O, and S elements on the catalysts. The surface acid concentration of the catalysts was determined by the acid-base inverse titration method. An excess NaOH solution (50 mL, 0.004 mol/L) was added to 0.1 g of catalyst in a small beaker at 25°C and allowed to stand for 30 min with sufficient stirring. The NaOH solution was neutralized with 0.004 mol/L HCl solution, and the solution pH was measured using a pH meter. The concentration of surface acid (C_{H+}) was calculated using the following formula:

$$C_{H+} = (V_{NaOH} \times C_{NaOH} - V_{HCl} \times C_{HCl}) / m_c$$

Of which, V_{NaOH} is the volume of NaOH solution added, C_{NaOH} is the concentration of NaOH standard solution, V_{HCl} is the volume of HCl solution consumed during titration, C_{HCl} is the concentration of HCl standard solution, m_{cat} is the mass of solid acid catalyst.

QUANTIFICATION AND STATISTICAL ANALYSIS

Our study doesn't include quantification or statistical analysis.